INORGANIC CHEMISTRY
FRONTIERS

RESEARCH ARTICLE

View Article Online
View Journal | View Issue

Cite this: *Inorg. Chem. Front.*, 2025, **12**, 8375

Ultrafast light-switch properties of a G-quadruplex binder: $[Ru(phen)_2(tpphz\text{-}DC3)]^{4+}$

Philip A. Morgenfurt,†[a] Avinash Chettri,†‡[b,c] Lorcan Holden,[a] Benjamin Dietzek-Ivanšić *§[b,c] and Tia E. Keyes *[a]

Received 24th July 2025,
Accepted 21st August 2025

DOI: 10.1039/d5qi01553g

rsc.li/frontiers-inorganic

Light-switch probes, where the probe only emits light on binding to its target, are highly attractive in bio-imaging as they provide for outstanding contrast, especially in the interrogation of a discrete and dynamic distributed structure like G-quadruplex DNA. Here, we examine the photophysical properties of a G-quadruplex (G4) selective probe comprising a light-switch Ru(II) dipyridylphenazine complex co-assembled with the well-known G4 selective ligand PDC3; $[Ru(phen)_2PDC3]^{4+}$ (**RuPDC3**), using femtosecond and nanosecond transient absorption spectroscopy, complemented by steady-state spectroscopy and spectro-electrochemistry. We compared the photophysics of RuPDC3 with that of a well-known photo-switch $[Ru(bpy)_2(dppz)]^{2+}$, **Rudppz**, and observed marked differences in their behaviours. Whereas in **Rudppz**, the ^{3}MLCT state is either localized on the phenanthroline or the phenazine unit, we show that in **RuPDC3**, this state has charge delocalised over the entire PDC3 unit. We then compared the ultrafast dynamics of this complex with **Rudppz** when associated with duplex and G4 DNA of different topologies and observed notable differences in trends in the exited-state dynamics in both **RuPDC3** and **Rudppz** with G4 for the first time. **RuPDC3** shows greater variation in excited-state dynamics with G4 topology and offers the prospect of elucidation of topology by ultrafast imaging.

Introduction

Ruthenium(II) polypyridyl complexes containing dppz = dipyrido[3,2-*a*:2′,3′-*c*]phenazine ligands are well known for their light-switch properties wherein their bright red emission in non-aqueous media is extinguished in H_2O and have been studied extensively in the literature.[1–11] Olson *et al.* were the first to hypothesize the existence of two competing emissive and non-emissive states in dppz-containing complexes as an explanation for this behaviour *i.e.*, a bright metal to ligand charge-transfer ($MLCT_{bright}$), and $MLCT_{dark}$ state. They proposed that in aprotic solvent, the $^3MLCT_{bright}$ state is populated by intersystem crossing (ISC) from the ^{1}MLCT state from where it deactivates *via* emission. In protic solvent, H-bonding to the phenazine moieties and solvent polarity reduce the energy of $MLCT_{dark}$ so that this state lies at lower energy than $MLCT_{bright}$ and it becomes the reservoir for excited state energy from which rapid non-radiative ground state recovery occurs.[1] Supported by significant evidence, both experimental and theoretical, their hypothesis that emission depends on dark and bright states that lie in variable degrees of equilibrium, depending on properties of the medium and temperature, is now widely accepted. Reported experimental data indicate that the dark state is associated with the phenazine portion of the dppz ligand while the bright state is centred on either the counter polypyridyl ligand or localised to the phen portion of the dppz ligand.[12,13] Regardless, some questions remain regarding the origin of the rapid deactivation mechanism of the dark state.[12–14]

Early studies attributed quenching of the dark state to H-bonding, excited-state proton transfer and/or the influence of the energy gap law on the deactivation of a low-energy dark state.[7,15–18] Currently, the most accepted explanation is that the dark state is quenched by bulk H_2O.[19] Exclusion of H_2O, leading to light-switch on, can be instigated by biomolecular recognition and so, for the past 30 years, ruthenium complexes containing the dppz ligand have found extensive applications in DNA detection, anticancer drugs, protein aggregation detection and as chemosensors.[17,20–34] For complexes like $[Ru(phen)_2(dppz)]^{2+}$ or $[Ru(bpy)_2(dppz)]^{2+}$, studies show that their binding affinity to B DNA is comparable to the classic interca-

[a]*School of Chemical Sciences, Dublin City University, Dublin 9, Ireland. E-mail: tia.keyes@dcu.ie*
[b]*Institute of Physical Chemistry, Friedrich Schiller University Jena, Helmholtzweg 4, 07743 Jena, Germany. E-mail: benjamin.dietzek@uni-jena.de*
[c]*Leibniz Institute of Photonic Technology (Leibniz-IPHT), Albert-Einstein-Straße 9, 07745 Jena, Germany*
† Both of these authors contributed equally.
‡ Current address: Institute of Physical Chemistry, University of Potsdam, Karl-Liebknecht-Straße 24-25, 14476 Potsdam, Germany.
§ Current address: Leibniz Institute of Surface Modification, Permoserstraße 15, 04318 Leipzig, Germany.

lator, ethidium bromide.[35–38] Recently, effort has been focussed on cell studies with a number of approaches taken to overcome the significant challenge of poor cellular uptake, and targeting of such complexes to regions of nucleic acid materials within cells.[39,40]

The dppz unit has been expanded into other ligand systems that also retain light switch behaviour on Ru(II) coordination. Ru(II) complexes of tpphz (tpphz = tetrapyrido[3,2-*a*:2′,3′-*c*:3″,2″-*h*:2‴,3‴-*j*]phenazine) show the same light-switch properties as dppz complexes. For example, luminescence of [Ru(bpy)$_2$(tpphz)]$^{2+}$ at 636 nm in dry acetonitrile is extinguished in H_2O.[41–45] Similarly, Ru-tpphz complexes are widely explored as DNA switches, including in living eukaryotic and prokaryotic cells, with the advantage that they were reported to be membrane penetrating without requirement for membrane permeabilization.[20,46–51] The tpphz ligand has also been widely explored as a bridge for dinuclear metal complexes.[41,42,52–54] There is increasing interest in developing probes that can discriminate non-canonical forms of DNA beyond duplex, including G-quadruplex (G4) and i-motif DNA structures. G4 structures are of particular biomedical interest.[55] G-quadruplex DNA form stacked guanine tetrads from guanine-rich DNA sequences under physiological conditions, through combined Hoogsteen base pair hydrogen bonding and stabilization through a central monovalent cation such as potassium or sodium.[56,57] Over 10 000 sequences in the human genome are predicted to be capable of forming G4 DNA structures under physiological conditions.[58,59] These sequences are highly prevalent in the telomere region of the human genome, near nucleosome-depleted regulatory regions close to transcription start sites of genes and in human oncogenes. G4s are believed to play a critical role in cancer and are also associated with genome expression and genome stability.[60–63] Molecular light-switches are particularly attractive for detection of such non-canonical structures for imaging and quantitation since the complexes will give a null signal in the absence of a target, in principle, emitting only when bound to G4, and this can lead to high-contrast imaging.[15,64] Ru-dppz- and dinuclear Ru-tppz-based complexes have been reported to show good affinity toward G4 in solution, and G4-binding induces the light-switch effect.[65] The first ultrafast studies of [Ru(phen)$_2$dppz]$^{2+}$ bound to both antiparallel and parallel G-quadruplex structures were reported recently and the differences in the complex's dynamics when bound to duplex *versus* G-quadruplex DNA were attributed to the influence of different water-binding patterns within the highly hydrated G-quadruplex structure.[57,66] However, Ru-dppz complexes typically do not show high specificity for duplex DNA.[57,67–69] Accordingly, efforts are ongoing toward adapting the Ru-dppz scaffold to improve its selectivity or to elicit emission responses that distinguish different DNA structures.[1,15,24,40,46,70] We recently reported a novel dppz ligand structure where we incorporated the well-known G4 ligand, PDC3, and prepared its coordination compound, [Ru(phen)$_2$(tpphz-DC3)]$^{4+}$ (Fig. 1a) where phen = 1,10-phenanthroline, tpphz = tetrapyrido[3,2-*a*:2′,3′-*c*:3″,2″-*h*:2‴,3‴-*j*]phenazine and DC3 = 2,9-diylbis(carbonylimino)bis[1-methylquinolinium]. The resulting complex exhibited preferential binding to G4 DNA, with affinity an order of magnitude greater than that for duplex DNA. Moreover, it offers clear discrimination between DNA and G4 on the basis of emission lifetime and resonance Raman signature.[70] These properties can, in principle, be discriminated *in cellulo* by imaging.

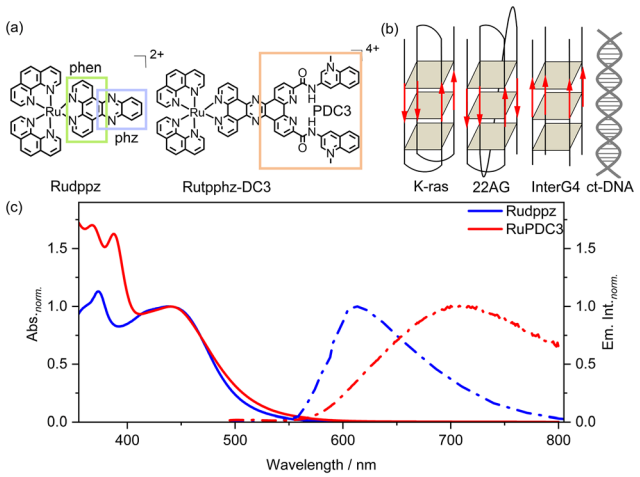

Fig. 1 (a) Chemical structures of **Rudppz** and **RuPDC3** investigated in this work. (b) A representative sketch showing the topology of the four DNA sequences formed in potassium phosphate buffer that were investigated in this work: K-ras, single strand antiparallel G-quadruplex (5′ AGGGCGGTGTGGGA-TAGGGAA 3′); 22AG, single strand hybrid G-quadruplex (5′ AGGGTTAGGGTTAGGGTTAGGG 3′); InterG4, parallel G-quadruplex, formed from four individual strands (5′ TAGGGT-TA 3′); and ct-DNA, duplex formed from two complementary strands (41.9 mol% G–C and 58.1 mol% A–T), where A is adenine, T is thymine, G is guanine and C is cytosine. The red arrows represent the direction from 5′ → 3′. (c) Steady-state absorption and emission spectra of **Rudppz** (blue) and **RuPDC3** (red) in acetonitrile. Emission spectra for both complexes are recorded at 450 nm excitation. All experiments are performed under aerated conditions.

As shown in Fig. 1c, the optical properties of [Ru(phen)$_2$(tpphz-PDC3)]$^{4+}$ are distinct from those of [Ru(phen)$_2$(dppz)]$^{2+}$. In particular, the emission spectrum from [Ru(phen)$_2$(tpphz-DC3)]$^{4+}$ shows a broad band red-shifted by more than 100 nm compared to that for [Ru(phen)$_2$(dppz)]$^{2+}$. Evidence from both experiment and theory indicates delocalisation of excited-state electron density across the extended tpphz-DC3 ligand and this may account for the impact of G4 on the photophysical changes induced on binding. In spite of this difference, the light-switch remains operational. In this contribution, we explore the photophysics of [Ru(phen)$_2$(tpphz-DC3)]$^{4+}$ (from here on referred to as **RuPDC3**) in solution (buffer and acetonitrile) and in G4-quadruplexes and duplex ct-DNA (Fig. 1b), with femtosecond and nanosecond transient absorption (fs- and ns-TA) spectroscopy. We compare the findings to the photophysics of the prototypical light-switch complex [Ru(phen)$_2$(dppz)]$^{2+}$ (from here on referred to as **Rudppz**), in solution and the DNA sequences used for **RuPDC3**, under identical conditions.

Experimental

Sample preparation

The synthesis of the ruthenium complexes has been described previously.[70] Chemicals were purchased from Sigma-Aldrich (Merck), Fischer Chemicals and CARL ROTH.

Femtosecond-TA and nanosecond-TA spectroscopy measurements were carried out in a 1 cm quartz cell under aerated conditions in distilled H_2O or acetonitrile (ACN). An optical density of 0.2–0.4 at 450 nm was used for all the measurements, corresponding to $[C]_{Ru}$ = 50 μM for both complexes. A power of ~0.2 mW was employed for fs-TA experiments, while ns-TA experiments were conducted at a power of ~2 mW. Analysis of the ns-TA spectra was completed using the sum of exponentials.[71]

For the SEC and CV measurements, a solution of $[C]_{Ru}$ = 0.8 mM was prepared in ACN with 0.1 M $TBAPF_6$. A solution of higher concentration, where $[C]_{Ru}$ = 1.2 mM, was prepared for the time-dependent SEC studies.

G4 DNA sequences were purchased from Eurofins Genomics and stored at −20 °C. The quadruplexes were prepared by following an established protocol obtained from a previously reported study.[72] Briefly, KPB buffer (10 mM potassium phosphate, 100 mM KCl) was used to anneal the quadruplex for all measurements. Quadruplexes were annealed at 95 °C for 10 min before cooling the solution slowly to room temperature over the span of 4 hours at $[C]_{Quad.}$ = 1 mM. Calf-thymus DNA (ct-DNA) was purchased from Merck and dissolved in PBS buffer to give a solution with $[C]_{ct\text{-}DNA}$ = 1 mM. Here $[C]_{Quad.}$ and $[C]_{ct\text{-}DNA}$ are expressed as the number of strands for G4 and number of base pairs for ct-DNA. The concentration of G4 was provided by the supplier, while for ct-DNA the concentration was determined *via* absorption at 260 nm and 280 nm in PBS before each experiment. Binding of ruthenium to DNA sequences was performed in a cuvette by adding ruthenium to DNA solution over 30 minutes, giving $[C]_{Ru}$ = 50 μM and $[C]_{Quad./ct\text{-}DNA}$ = 80 μM.[73] At these concentrations, complete binding of the complex to the DNA is ensured.[70] In order to ensure stability of the sample, solutions were checked for photo-bleaching and photo-product formation after each measurement, by comparing the absorption spectra before and after the experiment. Neither of these two processes was observed.

Steady-state UV-vis absorption and emission spectroscopy

UV-visible (UV-vis) absorption spectra were recorded using a Jasco-V760 spectrophotometer and emission spectra were recorded using an FLS980 spectrometer (Edinburgh Instruments) in a 1 cm quartz cell.

Femtosecond and nanosecond transient absorption (fs-TA and ns-TA) spectroscopy

A complete description of the fs-TA set up was provided elsewhere.[74,75] In brief, the 800 nm fundamental output of an amplified Ti:sapphire laser was split into two portions, where one portion was passed through a barium borate (BBO) crystal to generate light of 400 nm wavelength while residual light from the other portion was focused on a rotating CaF_2 plate to generate the white light continuum. The delay time used in this study was 1.8 ns. The mutual polarization between pump and probe was set to the magic angle (~54.7°).

For nanosecond transient absorption spectroscopy experiments, 450 nm pump pulses were generated from an optical parametric oscillator (OPO), pumped by a 10 Hz Nd:YAG laser with time resolution of ~10 ns. The probe light was generated from a xenon arc lamp. Transient absorption signals were detected by using a commercially available system acquired from Princeton Instruments.

Spectro-electrochemistry (SEC)

SEC experiments were carried out using a CHI 900 potentiostat coupled to a V-670 spectrophotometer (Jasco) with Ag/Ag^+ as the reference electrode, Pt gauze as the optically transparent working electrode, and Pt wire as the counter electrode. Studies were conducted in ACN with 0.1 M tributylammonium hexafluorophosphate ($TBAPF_6$) as a supporting electrolyte. SEC and voltammetric measurements were carried out in a quartz spectro-electrochemical cell (IJ Cambria) with a 1 mm optical path length. Cyclic voltammetry was carried out in the ranges of 0 to 1.3 V and 0 to −1.8 V. For SEC, a potential of 1.09 V was applied and time-dependent spectra were recorded from 0 to 40 minutes.

Results & discussion

Photophysics of Rudppz and RuPDC3 in H_2O and acetonitrile

Fig. 1c shows the steady-state UV-vis absorption spectra of **Rudppz** and **RuPDC3** in ACN. In **Rudppz**, the absorption bands at 373 nm and 440 nm correspond to ligand-based π–π* and metal-to-ligand charge-transfer (MLCT) transitions, respectively.[1,76]

For **RuPDC3**, an additional band at 388 nm is observed that is attributed, from previously reported computation, to an intra-ligand charge-transfer (ILCT) transition between the phenanthroline and the methylquinolinium pendants of the heteroligand.[70] The ^{1}MLCT absorption signals for **RuPDC3** and **Rudppz** are comparable, although the absorption is red-shifted and broader for **RuPDC3**. This is due to two contributing transitions from the highest occupied molecular orbital (HOMO) of the Ru(II) centre to the unoccupied molecular orbital of the phen and the terminal methylquinolinium on PDC3.[70] Fig. 1c also shows the emission spectra of **RuPDC3** and **Rudppz** in ACN. For **Rudppz**, the luminescence in ACN is centred at 613 nm and attributed to ^{3}MLCT phen-based emission.[1] Similar to the absorbance, the emission from **RuPDC3** is broader with a greater Stokes shift and maximum at 710 nm. Compared to **Rudppz**, the **RuPDC3** emission is red-shifted by 2230 cm^{-1}. This is, from computation, due to delocalization of the excited state over the extended π system of the PDC3, with the emission attributed to a $^3MLCT_{tpphz\text{-}DC3}$-based state (*vide infra*). Like **Rudppz**, **RuPDC3** behaves as a light-

switch. Its emission is extinguished in H_2O, indicating that H-bonding to the pyrazine of tpphz leads to population of a dark state. The photophysics of **Rudppz**-related complexes has been widely studied.[1,9,37,57,75,77–80] Since the photophysical properties of **Rudppz** are of fundamental importance to understand the photophysics of the light-switch behaviour of **RuPDC3**, we performed time-resolved spectroscopy of **Rudppz** in H_2O and ACN for comparison.

Fig. S1 shows the femtosecond transient absorption (fs-TA) spectra and kinetics of **Rudppz** in H_2O upon 400 nm excitation. The spectra (Fig. S1a) are composed of excited-state absorption (ESA) features below 377 nm and above 515 nm, while a ground-state bleach (GSB) dominates between 377 and 515 nm.[1] At a delay time of 1 ps, the differential absorption spectrum is composed of a broad ESA above 515 nm and a sharp ESA band with a maximum at 355 nm, highly reminiscent of the TA features of $[Ru(bpy)_3]^{2+}$ and $[Ru(phen)_3]^{2+}$.[78–80] The 355 nm ESA is associated with a $^3MLCT_{phen}$ state, from LC transitions within the reduced phen moiety, whereas the broad ESA above 515 nm stems from a combination of ligand-to-metal charge-transfer (LMCT) and ligand-centred (LC) transitions.[1,57,78–80] Within 20 ps, the ESA intensity above 625 nm decays, concomitant with an increase of the ESA maximum at 565 nm. This feature is comparatively sharper than the one observed at 1 ps and is associated with a non-emissive $^3MLCT_{phz}$-based state.[1,57] At longer delay times, an overall decrease in ESA and GSB signal is observed (Fig. S1b). Global kinetic analysis, applying a sum of two exponentials, yields two time constants: τ_1 = 2.5 ps and τ_2 = 250 ps (Fig. S1c).[75] These values agree with previously reported values in the literature determined by, for example, Olson *et al.*[1] τ_1 is associated with a decrease and an increase in ESA above and below 575 nm, respectively, and is therefore assigned to the $^3MLCT_{phen} \rightarrow {}^3MLCT_{phz}$ transition.[1,57] τ_2 decreases the ESA and GSB simultaneously and is therefore associated with molecules repopulating the ground state, *i.e.*, the $^3MLCT_{phz} \rightarrow S_0$ transition. For comparison, Fig. S5b shows the fs-TA kinetics of **Rudppz** in ACN upon 400 nm excitation. The kinetics at 450 nm and 560 nm, which are associated with GSB and ESA, respectively, do not undergo significant changes within the temporal window of the experiment (~1.8 ns). This is because in ACN, the $^3MLCT_{phz}$-based state is destabilized, so the $^3MLCT_{phen}$ is the lowest-lying state, with a lifetime of 180 ns, *i.e.*, the light-switch phenomenon is turned on in this medium.[37]

Fig. 2 shows the fs-TA spectra and kinetics of **RuPDC3** in H_2O at 400 nm excitation. The fs-TA spectrum recorded at 1 ps is dominated by excited-state absorption (ESA) below 368 nm and above 522 nm, with ground-state bleach (GSB) in between (Fig. 2a). The ESA observed closely resembles the features typically associated with the $^3MLCT_{phen}$-based state.[77,79,80] Within 7 ps, this band decreases with concomitant formation of an ESA with a maximum at 617 nm. This ESA band is absent in the spectra of **Rudppz** (*vide supra*) and $[Ru(tbbpy)_2(tpphz)]^{2+}$ and therefore stems from the charge-transfer from phen to PDC3, *i.e.*, a $^3MLCT_{phz\text{-}PDC3}$ state.[81]

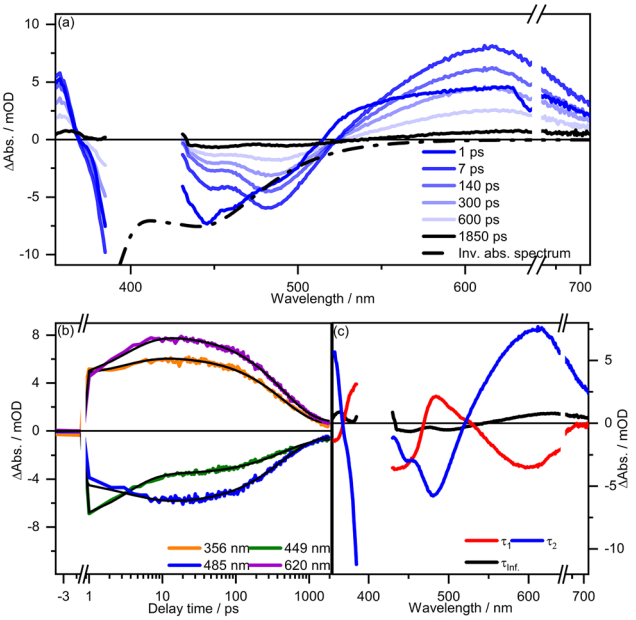

Fig. 2 Femtosecond transient absorption (fs-TA): (a) spectra, (b) kinetics and (c) decay-associated spectra of **RuPDC3** in H_2O, at 400 nm excitation. Imposed on the spectra in (a) is the inverted steady-state absorption of **RuPDC3** in H_2O. All experiments are performed under aerated conditions. The break in the wavelength-axis indicates the spectral region where an artifact is present.

The charge-transfer process is also associated with an increase in GSB at 480 nm, which corresponds to $MLCT_{phz\text{-}PDC3}$ bleach with a concomitant decrease in GSB below 470 nm. This is followed by a near-complete decay of the signals associated with both GSB and ESA within 1.8 ns (Fig. 2b). In Ru-based complexes, intersystem crossing (ISC) from $^1MLCT \rightarrow {}^3MLCT$ takes place in less than 100 fs, promoted by the presence of the heavy Ru ion.[9,77,78] Our current instrumental resolution of ~120 fs precludes direct investigation of ISC; therefore the excited-state dynamics originating from the ^3MLCT state is investigated. The experimental kinetics is analysed by global fitting employing a sum of two exponentials with characteristic time constants of τ_1 = 0.6 ps and τ_2 = 435 ps (Fig. 2c). τ_1 leads to a decrease in ESA at 360 nm and 510 nm as well as a decrease in GSB at 450 nm with a simultaneous build-up of GSB at 480 nm. We associated this process with a charge-transfer from the phen unit to the phz-PDC3 unit, *i.e.*, $^3MLCT_{phen} \rightarrow {}^3MLCT_{phz\text{-}PDC3}$. DAS of τ_2 manifests as an overall loss of GSB and ESA, without the formation of a new band, indicating ground state recovery, assigned to $^3MLCT_{phz\text{-}PDC3} \rightarrow S_0$. Therefore, our findings show that the photophysics of **RuPDC3** in H_2O is governed by an ultrafast deactivation of the ^3MLCT state, *i.e.*, a scenario similar to that observed in **Rudppz**, but with electron density delocalised over the PDC3 units.

Fig. 3 shows fs-TA spectra and the kinetics of the **RuPDC3** in ACN. As in H_2O, in ACN, a broad differential absorption signal at 1 ps is observed, which reveals the characteristic fea-

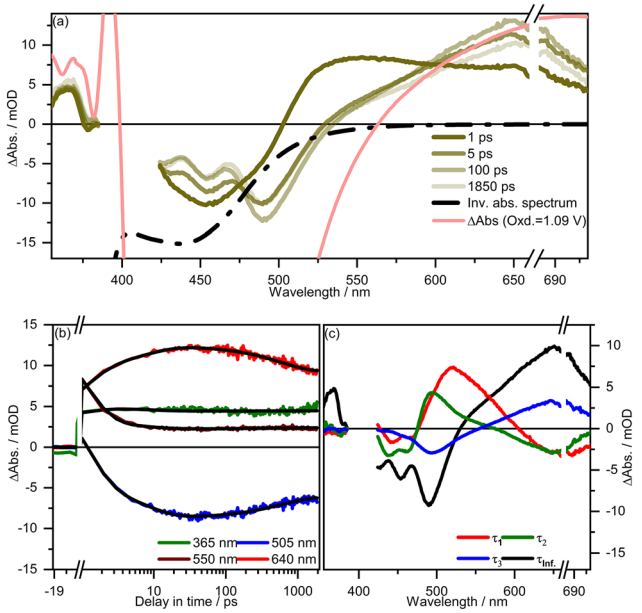

Fig. 3 Femtosecond transient absorption (fs-TA): (a) spectra, (b) kinetics and (c) decay-associated spectra of **RuPDC3** in acetonitrile (ACN), at 400 nm excitation. Imposed on the spectra in (a) is the inverted steady-state absorption while Δabsorbance (1.09 V–0 V) is indicated by the overlayed SEC-spectrum of **RuPDC3** in ACN using a 1.09 V potential. fs-TA experiments are performed under aerated conditions whereas spectro-electrochemistry experiments are performed under inert conditions. A break in the wavelength-axis indicates the spectral region where an artifact is present.

tures of the ^{3}MLCT$_{phen}$-based state (Fig. 3a).[77,79,80] Within 5 ps, the ^{3}MLCT$_{phen}$ band evolves into an ESA feature with a maximum at 650 nm that is associated with the ^{3}MLCT$_{phz\text{-}PDC3}$-based state (see the SEC section for assignments, *vide supra*), following which, the band exhibits a minor decay in ESA with no observable decrease in GSB at 440 nm (Fig. 3b). The ESA band is red-shifted in ACN compared to H_2O due to the differences in stabilization of the charge-separated ^{3}MLCT$_{dppz\text{-}PDC3}$ state. An additional time constant is required to fit the fs-TA kinetics of **RuPDC3** compared to **Rudppz**. A tri-exponential fit with an infinite component (τ_1 = 0.5 ps, τ_2 = 3 ps and τ_3 = 590 ps) is used for fitting the data in ACN (Fig. 3c). τ_1 leads to a decrease and an increase in ESA at 540 nm and 650 nm, respectively, with an increase in GSB at 488 nm (corresponding to MLCT$_{phz\text{-}PDC3}$ bleach). Therefore, we associate τ_1 with the ^{3}MLCT$_{phen}$ → ^{3}MLCT$_{phz\text{-}PDC3}$ transition. τ_2 exhibits spectral features similar to τ_1 but with a slight blue-shift of the ESA maximum. Such shifts correspond to relaxation of molecules to the lowest vibrational quanta from higher vibrational levels of the potential energy surface of the excited state. Therefore, τ_2 is associated with vibrational cooling within the ^{3}MLCT$_{phz\text{-}PDC3}$ manifold, *i.e.*, ^{3}MLCT$_{phz\text{-}PDC3(hot)}$ → ^{3}MLCT$_{phz\text{-}PDC3(cool)}$. τ_3 leads to an overall decrease in the ESA at 650 nm with no significant change in GSB. Instead, the decrease at 650 nm leads to a concomitant increase in ESA at 365 nm, which is typically associated with the ^{3}MLCT$_{phen}$ state. Thus, we conclude that the process associated with τ_3 leads to an increase in negative charge density at the phen moiety coordinated to Ru(II), due to partial delocalization of charge within the dppz-PDC$_3$ ligand *i.e.*, ^{3}MLCT$_{phz\text{-}PDC3}$ → ^{3}MLCT$_{dppz\text{-}PDC3}$. $\tau_{Inf.}$ corresponds to the offset of the fits, indicating that the ^{3}MLCT$_{dppz\text{-}PDC3}$-based state is long-lived and persists after 1.8 ns. This state is emissive and decays with a lifetime of 90 ns as shown in nanosecond transient absorption (ns-TA) spectra (Fig. S2).

To further validate the assignment of the ESA feature observed at 650 nm in ACN to the ^{3}MLCT$_{phz\text{-}PDC3}$ state, cyclic voltammetry (Fig. S3a) and UV-vis spectro-electrochemical (SEC) studies were conducted on **RuPDC3** (Fig. S3 in the SI). Cathodic processes are observed at peak potentials of −1.1 V and −1.6 V associated with ligand reduction, and a reversible oxidative process at 1.09 V *vs.* Ag/Ag$^+$ attributed to the Ru(II)/(III) couple. UV-vis SEC carried out at the peak potential of 1.09 V shows a decrease in the ^{1}MLCT absorption with the formation of a broad band extending from 600–800 nm. This is similar to the TA spectrum observed in ACN at 5 ps (see, Fig. 3a) and is attributed to PDC3 → Ru(III) *i.e.*, a ligand to metal charge-transfer transition, consistent with the assignment of the ESA at 617 nm in H_2O and 650 nm in ACN (see, Fig. 2 and 3) to the ^{3}MLCT$_{phz\text{-}PDC3}$ state.

Excited-state dynamics of Rudppz and RuPDC3 in DNA

We recently reported that **RuPDC3** showed an order of magnitude greater binding affinity for quadruplex over duplex DNA, with variation of affinity over different G4 topologies.[70] Steady-state emission spectroscopy confirmed the light-switch behaviour of **RuPDC3** on binding to G4-quadruplexes and duplex DNA, albeit with a weaker effect in duplex DNA. Correspondingly, time correlation single photon counting (TCSPC) showed distinct differences in emission lifetimes and amplitudes of **RuPDC3** bound to duplexes and G4-quadruplexes. These findings raised questions in relation to the differences in the ultrafast excited-state dynamics of **Rudppz** and **RuPDC3**, in G4-quadruplexes of different, but well characterised topology.[70] Here, we investigated the association of both complexes with G-quadruplex sequences representating different topologies (see Fig. 1b). These included (i) 22AG, a 22-mer human telomeric sequence known for its polymorphic behaviour, forming mixed hybrid quadruplex structures in solution; (ii) K-ras, a promotor-derived sequence that adopts a parallel G-quadruplex topology; and (iii) d(TAGGGTTA), a sequence that forms an intermolecular parallel G-quadruplex structure, referred to hereafter as InterG4.[68,82,83] As well, for comparison, the complexes on association with duplex calf thymus DNA (ct-DNA) were also studied. In all experiments, a constant ratio of $[C]_{DNA}/[C]_{Ru}$ = 1.8 is maintained, which corresponds to saturated binding of the complex, *i.e.*, a scenario in which the emission intensity does not change with further addition of DNA. Given $[C]_{Ru}$ = 50 μM and $[C]_{DNA}$ = 80 μM along with known binding constant (K_b) values in G4-quadruplexes (10^7 M^{-1}) and ct-DNA (10^6 M^{-1}), it is safe to conclude that, under these experimental conditions, nearly all Ru-

complexes are bound to the DNA.[70] To ensure studies were completed under equilibrium binding conditions, the solutions were incubated with stirring for 30 minutes prior to performing fs-TA and ns-TA experiments, and we confirmed that no spectral changes occurred beyond this window. For experiments with quadruplexes, a potassium phosphate buffer (KPB) with KCl is used whereas a sodium phosphate buffer (PBS) is used for ct-DNA (see the Sample preparation section).

fs-TA of Rudppz interacting with DNA

Although ultrafast dynamics of **Rudppz** in duplex and some G4 DNA have been reported previously,[10,57,59] we have completed similar studies here to facilitate comparison with **RuPDC3** under identical experimental conditions. Furthermore, the ultrafast spectroscopy of **Rudppz** with the specific G4 structures examined here have not been recorded previously. Fig. 4 shows fs-TA spectra, kinetics and DAS of **Rudppz** in K-ras upon 400 nm excitation. At short delay times of 1 ps, excited-state absorption (ESA) features appear below 370 nm and above 510 nm, while a ground-state bleach (GSB) dominates between 370 and 510 nm (Fig. 4a and b). The features observed at 1 ps are notably similar to those observed in H_2O and ACN (*vide supra*) and are thus assigned to the $^3MLCT_{phen}$ state. Upon increasing the delay time from 1 ps to 5 ps, an ESA with a maximum at 550 nm (associated with the $^3MLCT_{phz}$ state) is formed at the expense of the ESA band observed at 1 ps (associated with the $^3MLCT_{phen}$ state), with no observable change in the GSB. This indicates a charge-transfer transition from phen to phz (τ_1 = 3 ps), *i.e.*, $^3MLCT_{phen} \rightarrow {}^3MLCT_{phz}$.

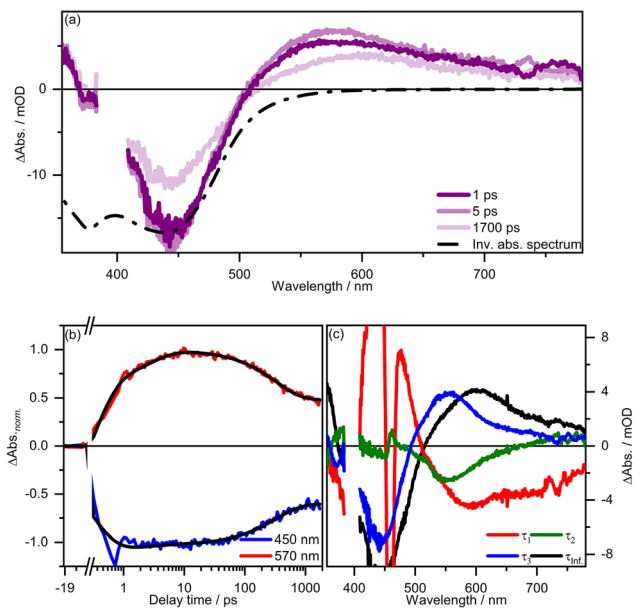

Fig. 4 Femtosecond transient absorption (fs-TA): (a) spectra, (b) kinetics and (c) decay-associated spectra of **Rudppz** in K-ras at 400 nm excitation. Imposed on the spectra in (a) is the inverted steady-state absorption of **Rudppz** in K-ras. The sharp band at 460 nm in (c) is due to the Raman band of H_2O. Experiments are performed under aerated conditions. A ratio of $[C]_{K\text{-}ras}/[C]_{Ru}$ = 1.8 is used where $[C]_{K\text{-}ras}$ is expressed as the number of strands.

The spectral change is followed by an overall decrease in the GSB and ESA, which is typically associated with repopulation of the ground state (τ_2 = 320 ps). However, at a delay time of 1850 ps, residual TA signatures remain, indicating the presence of a long-lived state whose decay kinetics cannot be accessed within the dynamic range of our experiment (~1.8 ns). Fitting of the kinetics yields the time constants τ_1 = 0.3 ps, τ_2 = 5 ps and τ_3 = 320 ps (Fig. 4c). τ_1 leads to the formation of a broad band above 510 nm, which resembles the spectral features of a ^{3}MLCT state. Therefore, the process is associated with formation of the $^3MLCT_{phen}$ state. τ_2 leads to a decrease in the ESA at 560 nm, which is associated with the $^3MLCT_{phen} \rightarrow {}^3MLCT_{phz}$ transition (for spectral assignment of $^3MLCT_{phen}$ and $^3MLCT_{phz}$ see Fig. S5 and its corresponding discussion). τ_3 leads to a partial decrease of GSB and ESA. This observation can be explained on the basis of two distinct sub-ensembles of **Rudppz** present in K-ras. The first sub-ensemble is composed of **Rudppz** bound to K-ras at sites that are relatively well exposed to H_2O molecules, leading to partial recovery of the excited molecules to the ground state (τ_2 = 320 ps). The other sub-ensemble is less exposed to H_2O, leading to a prolonged lifetime of 50 and 300 ns (see Fig. S3). Our finding is consistent with previous studies, which show supressed population of the $^3MLCT_{phz}$ state in **Rudppz** bound to ct-DNA and other quadruplex structures, since intercalation of the complex protects the phenazine from H_2O.[57,84,85] However, in some of the complexes, dark $^3MLCT_{phz}$ states are populated to varying extents, depending on the different binding orientations that modulate the degree of phenazine exposure to water. This is supported by multiple studies.[39,57,70,86] Here, it is also important to note that, like other studies, racemic complexes are used and so the subpopulations may originate from differential enantiomer binding at the G4 structures. The fs-TA spectra and kinetics of **Rudppz** associated with InterG4 and ct-DNA, as shown in Fig. S4, closely resemble those described above for the complex with K-ras, so we focussed here on the description of the dynamics for K-ras as being representative of all three. The behaviour also corresponds well with that reported recently for an anti-parallel human telomere G4 structure.[57] Interestingly, a notable outlier amongst the investigated DNA topologies is the excited-state dynamics of **Rudppz** with 22AG (Fig. 5). Composed of a GSB between 370 nm and 510 nm with ESA on either side, the TA spectra of **Rudppz** in 22AG do not undergo significant changes in the GSB and ESA above 1 ps and closely resemble the excited-state dynamics result of the complex in ACN (Fig. S1). This indicates that the **Rudppz** binding orientation(s) at this G4 topology is well shielded from H_2O, leading to a near-complete population of the long-lived and emissive $^3MLCT_{phen}$ state. This is consistent with the large emission intensity enhancements on binding to 22AG reported previously.[87]

fs-TA of RuPDC3 in DNA

Fig. 6 shows the fs-TA spectra, kinetics and DAS of **RuPDC3** with K-ras at 400 nm excitation. At 0.7 ps, the fs-TA spectrum

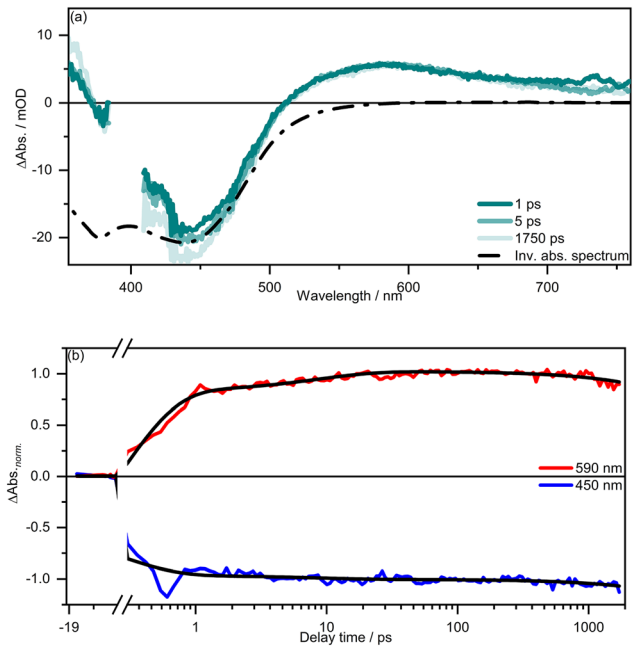

Fig. 5 Femtosecond transient absorption (fs-TA): (a) spectra and (b) normalized kinetics of **Rudppz** in 22AG at 400 nm excitation. Imposed on the spectra in (a) is the inverted steady-state absorption of **Rudppz** in 22AG. Experiments are performed under aerated conditions. A ratio of $[C]_{22AG}/[C]_{Ru}$ = 1.8 is used where $[C]_{22AG}$ is expressed as the number of strands.

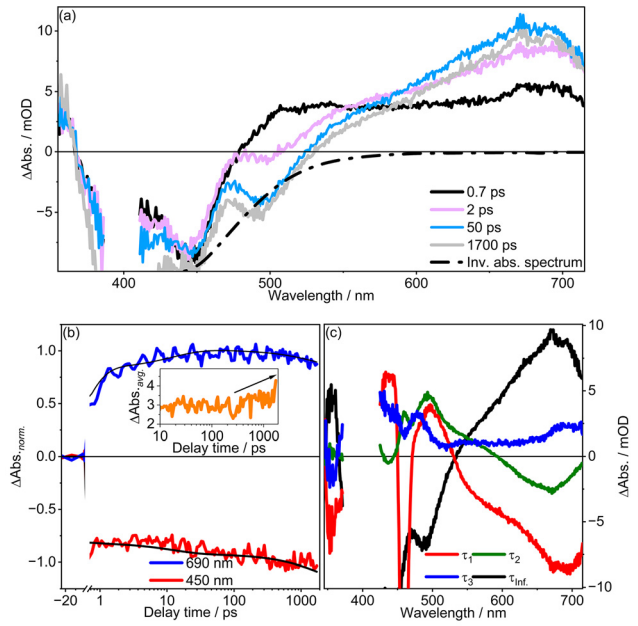

Fig. 6 Femtosecond transient absorption (fs-TA): (a) spectra, (b) normalized kinetics and (c) decay-associated spectra of **RuPDC3** in K-ras at 400 nm excitation. Imposed on the spectra in (a) is the inverted steady-state absorption of **RuPDC3** in K-ras. In (b), the kinetics shown in the inset corresponds to an averaged kinetic trace from 355 to 365 nm, showing an increase in signal after 100 ps. The sharp band at 460 nm in (c) is due to the Raman band of H_2O. Experiments are performed under aerated conditions. A ratio of $[C]_{K\text{-}ras}/[C]_{Ru}$ = 1.8 is used where $[C]_{K\text{-}ras}$ is expressed as the number of strands.

is composed of ESA below 368 nm and above 470 nm with a GSB in between. At this time delay, a broad featureless ESA dominates above 522 nm, characteristic of a $^3MLCT_{phen}$ state.[77,79,80] Within 2 ps, the $^3MLCT_{phen}$ band decreases with concomitant formation of an ESA with a maximum at 680 nm, which is associated with the formation of the $^3MLCT_{phz\text{-}PDC3}$ state (τ_1 = 0.5 ps). The transition is also marked by a shift in the GSB maximum from 450 nm to 490 nm. At 50 ps, the ESA band is comparatively sharper than it is at 5 ps. This indicates vibrational relaxation within the $^3MLCT_{phz\text{-}PDC3}$ manifold (τ_2 = 3 ps). At very long delay times, *i.e.*, 1850 ps, a slight decrease in the ESA (~8.3%) above 535 nm is observed with no discernible decrease in the GSB. As described for **RuPDC3** in ACN (see Fig. 3), here too the ESA at 365 nm (associated with the $^3MLCT_{phen}$ state) builds up at the expense of the ESA at 680 nm (associated with the $^3MLCT_{PDC3}$ state) at delay times above 100 ps (inset, Fig. 6b). Fig. 7 shows a comparison of fs-TA spectra and kinetics of **RuPDC3** in the G4s and ct-DNA. In all DNA sequences, the process of $^3MLCT_{phen} \rightarrow {}^3MLCT_{phz\text{-}PDC3}$ is observed within 2 ps, followed by blue-shifting of the ESA band within 50 ps, indicating vibrational cooling. At longer delay times, a decrease in the ESA at 690 nm is observed in all cases while no discernible change in GSB at 450 nm for duplex, K-ras and InterG4 is observed. For 22AG, kinetic traces show a decrease in GSB at 450 nm. As stated earlier, the spectral change in duplex, K-ras and InterG4 is hypothesized to be due to different extents of charge delocalization across the PDC3 ligand due to differences in relative orientation of the terminal bisquinolinium moieties when the complex is bound to duplex and different quadruplex topologies. Varying the binding orientation of **RuPDC3** will also result in varying exposure to water. However additional experiments are required to fully validate this theory.

Interestingly, the dynamics observed above 50 ps for 22AG indicates a faster ground state repopulation for **RuPDC3** when bound to this quadruplex. This indicates that, within 22AG, the binding environment is significantly different for **RuPDC3** compared to the other DNA sequences. This is consistent with our earlier observations *via* circular dichroism (CD),[70] wherein **RuPDC3** showed distinctive behaviour when bound to 22AG compared to other quadruplexes. Whilst the other quadruplexes showed evidence of structural disruption on **RuPDC3** binding, with 22AG, rather than disruption of the quadruplex structure, a conformational change to an antiparallel quadruplex was indicated. This is also consistent with other literature reports on PhenCD3 where structures analogous to 22AG refolded to an antiparallel structure on ligand binding.[70,88,89] Overall, our findings indicate that the $^3MLCT_{dppz\text{-}PDC3}$ state in **RuPDC3** is formed within 5 ps. While the photophysics is similar to that of **Rudppz**, it is significantly more complex in **RuPDC3**, especially in relation to the excited-state dynamics between 100 and 1800 ps.

Ns-TA of RuPDC3 in DNA

In order to characterize the long-lived states for **RuPDC3** on its association with DNA, we performed ns-TA spectroscopy. The time-constants for the different photophysical processes,

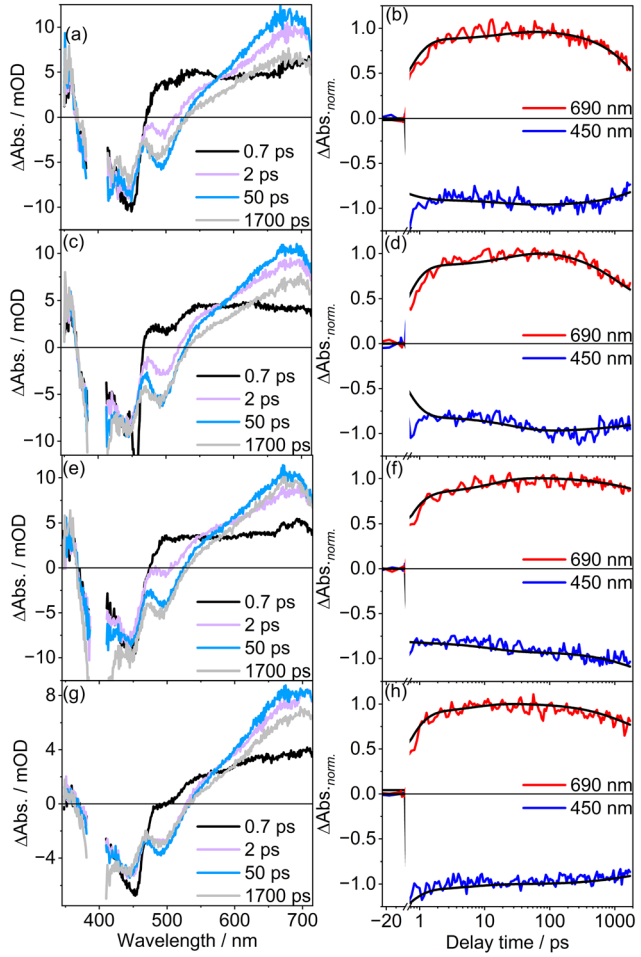

Fig. 7 Femtosecond transient absorption spectra and normalized kinetics of **RuPDC3** in (a and b) 22AG, (c and d) InterG4, (e and f) K-ras and (g and h) ct-DNA, at 400 nm excitation. Experiments are performed under aerated conditions. A ratio of $[C]_{DNA}/[C]_{Ru}$ = 1.8 is used where $[C]_{DNA}$ is expressed as the number of strands for G-quadruplexes and as the number of base-pairs for ct-DNA.

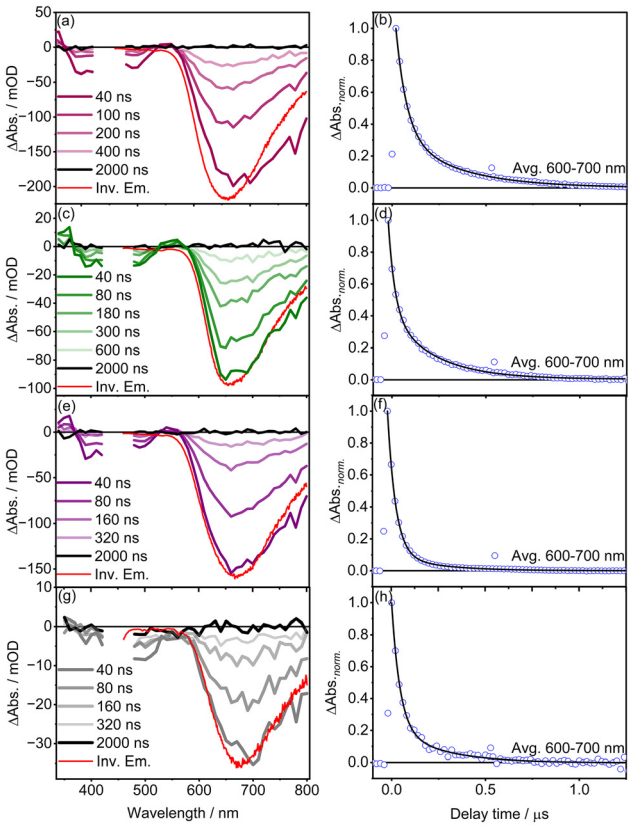

Fig. 8 Nanosecond transient absorption (ns-TA) spectra and normalized kinetics of **RuPDC3** in (a and b) 22AG, (c and d) InterG4, (e and f) K-ras and (g and h) ct-DNA, at 450 nm excitation. Imposed on ns-TA spectra is the inverted steady-state emission spectrum at 450 nm excitation. The kinetics shown are averaged from 600–700 nm. Experiments are performed under aerated conditions. A ratio of $[C]_{DNA}/[C]_{Ru}$ = 1.8 is used where $[C]_{DNA}$ is expressed as the number of strands for G-quadruplexes and as the number of base-pairs for ct-DNA.

across femto and nano-time domain experiments for **RuPDC3** in association with the four DNA sequences, are summarized in Table S1.

Since ns-TA spectra and kinetics of **RuPDC3** in all G4-quadruplexes and ct-DNA are similar, we discuss the photophysics together. Fig. 8 shows the ns-TA spectra and kinetics of **RuPDC3** in the DNA sequences. In all sequences, at 40 ns, the TA spectrum of **RuPDC3** resembles GSB between 370 nm and 430 nm and a ^{3}MLCT-ESA band with a maximum at 365 nm and the typical ^{3}MLCT absorption signal above 530 nm are observed. The ns-TA kinetics is modelled with a biexponential function that yields time constants between 45 and 60 ns and between 240 and 320 ns in all DNA sequences (see Table S1). The dual lifetime reflects the presence of two distinct ensembles of **RuPDC3** within the DNA.[71] Across DNA topologies the ns-lifetimes are similar, but the fraction of molecules contributing to the two distinct ensembles (ensemble 1 and 2) vary with topology. In ct-DNA and K-ras, the ensemble with lifetime in the 45–60 ns range (ensemble 1) has a weighted coefficient (A_1) of 80%, whereas the remaining 20% of molecules constitutes ensemble 2. In InterG4 and 22AG, both ensembles of **RuPDC3** contribute equally. While it is difficult to predict structurally what the two distinct ensembles correspond to, it is likely that they represent distinct binding of **RuPDC3** enantiomers to the DNA sequences (as a racemic mixture is used). Ns-TA of **Rudppz** in DNA also showed biexponential decay kinetics, indicating the presence of distinct binding sites (Fig. S5).

Conclusions

We investigated the photophysics of **Rudppz** and the G4-quadruplex-selective photoswitch **RuPDC3** across solution, duplex DNA and G4-quadruplex DNA environments spanning fs to ns timescales. Studies were complemented by spectro-electrochemistry. The key findings are summarised as a simplified Jablonski diagram, as shown in Fig. 9. Consistent with pre-

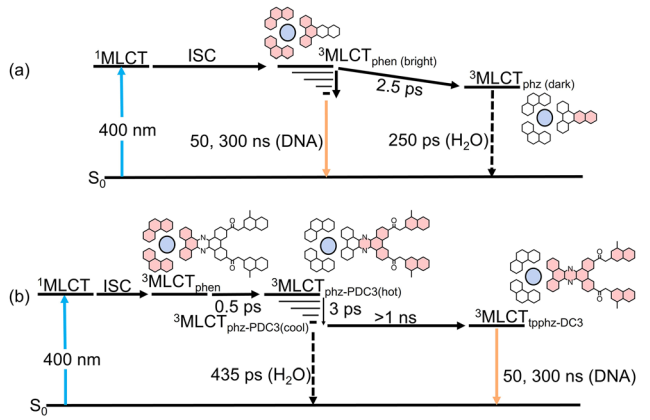

Fig. 9 A simplified Jablonski diagram depicting the photophysics of (a) **Rudppz** and (b) **RuPDC3** in H_2O and DNA. Of note is the light-switch effect observed in both complexes in DNA. Colouring in red indicates regions in the PDC3 ligand where electron-density resides after charge separation, whereas colouring in blue indicates the oxidized Ru(III) centre.

vious reports, **Rudppz** shows ultrafast deactivation from a stabilized non-emissive $^3MLCT_{phz}$-based state in H_2O. In ACN, repopulation of the ground state occurs from an emissive $^3MLCT_{phen}$-based state with a lifetime of 650 ns.[90] We demonstrate that light-switch behaviour is also operative in **RuPDC3**. However, based on differences in the ESA between **Rudppz** and **RuPDC3** and the SEC of **RuPDC3** in ACN, we conclude that the lowest-lying state in **RuPDC3** is $^3MLCT_{phz\text{-}PDC3}$-based with the electron density delocalized across the entire ligand, confirming previous theoretical predictions.[84] In H_2O, the $^3MLCT_{phz\text{-}PDC3}$ state is dark and undergoes ultrafast deactivation with a lifetime of 435 ps whereas in ACN, the absence of H-bonding with nitrogen atoms of phenazine (phz) leads to prolonged emission with a lifetime of 50 and 300 ns, which arises from a bright $^3MLCT_{dppz\text{-}PDC3}$-based state. The "light-switch" induction observed for **Rudppz** in ct-DNA and G4-quadruplexes also occurs for **RuPDC3**. However, interestingly, we observed that the dynamics of the excited state photophysics varied for each complex with different G-quadruplex structures.

fs-TA spectroscopy of **Rudppz** showed distinct photophysics in mixed hybrid 22AG compared to ct-DNA and the other quadruplexes. While the formation of the $^3MLCT_{phen}$ state occurs in **Rudppz** within 2 ps for all the DNA sequences, a partial ground-state recovery is observed in K-ras, InterG4 and ct-DNA. This is not the case in 22AG, where no ground state recovery is observed within the experimentally accessible time window indicating effective exclusion of water when **Rudppz** is associated with this quadruplex. In the case of **RuPDC3**, the $^3MLCT_{phz\text{-}PDC3}$ state is populated within 2 ps for all DNA sequences studied followed by vibrational relaxation within 50 ps. Notably, **RuPDC3** showed a distinct response compared to **Rudppz**. When bound to 22AG, **RuPDC3** shows partial ground state recovery indicating a different binding mode to this quadruplex, whereas in InterG4, ct-DNA and K-ras only a nominal change in GSB at 450 nm was observed, indicating effective water exclusion in the binding orientation of **RuPDC3**. For both **RuPDC3** and **Rudppz**, a dual emission is observed in all DNA sequences in the ns range. This suggests two distinct coordination environments for the complexes with the quadruplex topologies explored. As the complexes are racemic mixtures, the distinct binding sites/geometries for each of the enantiomers of the complexes may contribute to this effect. This is an open question that we hope to address in future work. The clear distinctions in photophysics of **Rudppz** and **RuPDC3** are attributed to the extended delocalisation of charge in the latter across the extended PDC3 portion of the ligand. The higher binding affinity of the latter for G4s compared to duplex DNA structures and differences in photophysical kinetics across G4 topologies, attributed to variation in binding environment, showcases its potential for *in cellulo* discrimination of different DNA structures with ultrafast imaging.

Author contributions

Philip Morgenfurt and Dr Avinash Chettri contributed equally to performing experiments, writing the original draft, reviewing and editing the manuscript. Dr Lorcan Holden prepared the complexes. Prof. Tia Keyes and Prof. Benjamin Dietzek-Ivanšić conceived the project and contributed to reviewing and editing the manuscript.

Conflicts of interest

There are no conflicts to declare.

Data availability

The data complementing the article have been included as a part of the SI. The following data are present in the SI: Figure S1. Fs-TA spectra, kinetics and DAS of **Rudppz** in H_2O and fs-TA kinetics in ACN, Figure S2. Ns-TA spectra and kinetics of **RuPDC3** in ACN, Figure S3. Cyclic voltammogram and spectro-electrochemistry of **RuPDC3** in ACN, Figure S4. Fs-TA spectra and kinetics of **Rudppz** in 22AG, InterG4, K-ras and ct-DNA, Figure S5. Ns-TA spectra and kinetics of **Rudppz** in 22AG, InterG4, K-ras and ct-DNA, Table S1. Time constants obtained from fitting the transient absorption kinetics of **RuPDC3** in different media with and without nucleic acid. See DOI: https://doi.org/10.1039/d5qi01553g.

Acknowledgements

A. C. and B. D. I. thank the Deutsche Forschungsgemeinschaft (German Research Foundation, project 395358570) for financial support. P. M., T. K. and L. H. gratefully acknowledge

Science Foundation Ireland under grant number [19/FFP/6428] and the Irish Research Council for funding.

References

1 E. J. C. Olson, D. Hu, A. Hörmann, A. M. Jonkman, M. R. Arkin, E. D. A. Stemp, J. K. Barton and P. F. Barbara, First Observation of the Key Intermediate in the "Light-Switch" Mechanism of [Ru(phen)$_2$ dppz^{2+}, *J. Am. Chem. Soc.*, 1997, **119**, 11458–11467.

2 J. C. Chambron, J. P. Sauvage, E. Amouya and P. Koffi, Ru (bipy)2(dipyridophenazine)2+: a complex with a long range directed charge transfer excited state, *Nouv. J. Chim.*, 1985, **9**, 527–529.

3 M. K. Kuimova, W. Z. Alsindi, J. Dyer, D. C. Grills, O. S. Jina, P. Matousek, A. W. Parker, P. Portius, X. Z. Sun, M. Towrie, C. Wilson, J. Yang and M. W. George, Using picosecond and nanosecond time-resolved infrared spectroscopy for the investigation of excited states and reaction intermediates of inorganic systemsBased on the presentation given at Dalton Discussion No. 6, 9?11th September 2003, University of York, UK., *Dalton Trans.*, 2003, 3996.

4 Y. Sun, Y. Liu and C. Turro, Ultrafast Dynamics of the Low-Lying ^{3} MLCT States of [Ru(bpy)$_2$ (dppp2)]$^{2+}$, *J. Am. Chem. Soc.*, 2010, **132**, 5594–5595.

5 C. G. Coates, J. J. McGarvey, P. L. Callaghan, M. Coletti and J. G. Hamilton, Probing the Interaction of [Ru(phen)$_2$ (dppz)]$^{2+}$ with Single-Stranded DNAWhat Degree of Protection Is Required for Operation of the "Light-Switch Effect"?, *J. Phys. Chem. B*, 2001, **105**, 730–735.

6 W. Chen, C. Turro, L. A. Friedman, J. K. Barton and N. J. Turro, Resonance Raman Investigation of Ru(phen)$_2$ (dppz)$^{2+}$ and Related Complexes in Water and in the Presence of DNA, *J. Phys. Chem. B*, 1997, **101**, 6995–7000.

7 C. Turro, S. H. Bossmann, Y. Jenkins, J. K. Barton and N. J. Turro, Proton Transfer Quenching of the MLCT Excited State of Ru(phen)2dppz2+ in Homogeneous Solution and Bound to DNA, *J. Am. Chem. Soc.*, 1995, **117**, 9026–9032.

8 M. K. Brennaman, T. J. Meyer and J. M. Papanikolas, [Ru (bpy)$_2$ dppz]$^{2+}$ Light-Switch Mechanism in Protic Solvents as Studied through Temperature-Dependent Lifetime Measurements, *J. Phys. Chem. A*, 2004, **108**, 9938–9944.

9 M. K. Brennaman, J. H. Alstrum-Acevedo, C. N. Fleming, P. Jang, T. J. Meyer and J. M. Papanikolas, Turning the [Ru (bpy)$_2$ dppz]$^{2+}$ Light-Switch On and Off with Temperature, *J. Am. Chem. Soc.*, 2002, **124**, 15094–15098.

10 C. Kuhnt, M. Karnahl, S. Tschierlei, K. Griebenow, M. Schmitt, B. Schäfer, S. Krieck, H. Görls, S. Rau, B. Dietzek and J. Popp, Substitution-controlled ultrafast excited-state processes in Ru–dppz-derivatives, *Phys. Chem. Chem. Phys.*, 2010, **12**, 1357–1368.

11 M. Schwalbe, M. Karnahl, S. Tschierlei, U. Uhlemann, M. Schmitt, B. Dietzek, J. Popp, R. Groake, J. G. Vos and S. Rau, The switch that wouldn't switch – unexpected luminescence from a ruthenium(II)-dppz-complex in water, *Dalton Trans.*, 2010, **39**, 2768.

12 C. G. Coates, J. Olofsson, M. Coletti, J. J. McGarvey, B. Önfelt, P. Lincoln, B. Norden, E. Tuite, P. Matousek and A. W. Parker, Picosecond Time-Resolved Resonance Raman Probing of the Light-Switch States of [Ru(Phen)$_2$ dppz]$^{2+}$, *J. Phys. Chem. B*, 2001, **105**, 12653–12664.

13 B. Önfelt, P. Lincoln, B. Nordén, J. S. Baskin and A. H. Zewail, Femtosecond linear dichroism of DNA-intercalating chromophores: Solvation and charge separation dynamics of [Ru(phen)$_2$ dppz]$^{2+}$ systems, *Proc. Natl. Acad. Sci. U. S. A.*, 2000, **97**, 5708–5713.

14 B. Önfelt, J. Olofsson, P. Lincoln and B. Nordén, Picosecond and Steady-State Emission of [Ru(phen)$_2$ dppz]$^{2+}$ in Glycerol: Anomalous Temperature Dependence, *J. Phys. Chem. A*, 2003, **107**, 1000–1009.

15 A. E. Friedman, J. C. Chambron, J. P. Sauvage, N. J. Turro and J. K. Barton, A molecular light switch for DNA: Ru(bpy) 2(dppz)2+, *J. Am. Chem. Soc.*, 1990, **112**, 4960–4962.

16 R. B. Nair, E. S. Teng, S. L. Kirkland and C. J. Murphy, Synthesis and DNA-Binding Properties of [Ru(NH$_3$)$_4$ dppz]$^{2+}$, *Inorg. Chem.*, 1998, **37**, 139–141.

17 T. Vlček, Preface "Controlling photophysical properties of metal complexes: Toward molecular photonics", *Coord. Chem. Rev.*, 2011, **255**, 2399–2400.

18 A. W. McKinley, P. Lincoln and E. M. Tuite, Environmental effects on the photophysics of transition metal complexes with dipyrido[2,3-a:3′,2′-c]phenazine (dppz) and related ligands, *Coord. Chem. Rev.*, 2011, **255**, 2676–2692.

19 A. A. Cullen, C. Long and M. T. Pryce, Explaining the role of water in the "light-switch" probe for DNA intercalation: Modelling water loss from [Ru(phen)2(dppz)]2+•2H$_2$O using DFT and TD-DFT methods, *J. Photochem. Photobiol., A*, 2021, **410**, 113169.

20 M. R. Gill and J. A. Thomas, Ruthenium(II) polypyridyl complexes and DNA—from structural probes to cellular imaging and therapeutics, *Chem. Soc. Rev.*, 2012, **41**, 3179.

21 L. Zeng, P. Gupta, Y. Chen, E. Wang, L. Ji, H. Chao and Z.-S. Chen, The development of anticancer ruthenium(II) complexes: from single molecule compounds to nanomaterials, *Chem. Soc. Rev.*, 2017, **46**, 5771–5804.

22 N. P. Cook, M. Ozbil, C. Katsampes, R. Prabhakar and A. A. Martí, Unraveling the Photoluminescence Response of Light-Switching Ruthenium(II) Complexes Bound to Amyloid-β, *J. Am. Chem. Soc.*, 2013, **135**, 10810–10816.

23 J. Tang, T. Yu, L. Guo, J. Xie, N. Shao and Z. He, In vitro selection of DNA aptamer against abrin toxin and aptamer-based abrin direct detection, *Biosens. Bioelectron.*, 2007, **22**, 2456–2463.

24 C. S. Burke, A. Byrne and T. E. Keyes, Targeting Photoinduced DNA Destruction by Ru(II) Tetraazaphenanthrene in Live Cells by Signal Peptide, *J. Am. Chem. Soc.*, 2018, **140**, 6945–6955.

25 A. Byrne, C. S. Burke and T. E. Keyes, Precision targeted ruthenium(II) luminophores; highly effective probes for cell imaging by stimulated emission depletion (STED) microscopy, *Chem. Sci.*, 2016, **7**, 6551–6562.

26 S. Rau, M. Schwalbe, S. Losse, H. Görls, C. McAlister, F. M. MacDonnell and J. G. Vos, Photoinduced Ligand Transformation in a Ruthenium Polypyridophenazine Complex, *Eur. J. Inorg. Chem.*, 2008, **2008**, 1031–1034.

27 E. Wachter, D. Moyá and E. C. Glazer, Combining a Ru(II) "Building Block" and Rapid Screening Approach to Identify DNA Structure-Selective "Light Switch" Compounds, *ACS Comb. Sci.*, 2017, **19**, 85–95.

28 E. Wachter, B. S. Howerton, E. C. Hall, S. Parkin and E. C. Glazer, A new type of DNA "light-switch": a dual photochemical sensor and metalating agent for duplex and G-quadruplex DNA, *Chem. Commun.*, 2014, **50**, 311–313.

29 C. Moucheron, A. Kirsch-De Mesmaeker and J. M. Kelly, Photoreactions of ruthenium(II) and osmium(II) complexes with deoxyribonucleic acid (DNA), *J. Photochem. Photobiol., B*, 1997, **40**, 91–106.

30 I. Ortmans, B. Elias, J. M. Kelly, C. Moucheron and A. Kirsch-DeMesmaeker, $[Ru(TAP)_2\ (dppz)]^{2+}$: a DNA intercalating complex, which luminesces strongly in water and undergoes photo-induced proton-coupled electron transfer with guanosine-5′-monophosphate, *Dalton Trans.*, 2004, 668–676.

31 I. Ortmans, C. Moucheron and A. Kirsch-De Mesmaeker, Ru(II) polypyridine complexes with a high oxidation power. Comparison between their photoelectrochemistry with transparent SnO2 and their photochemistry with desoxyribonucleic acids, *Coord. Chem. Rev.*, 1998, **168**, 233–271.

32 G. Pourtois, D. Beljonne, C. Moucheron, S. Schumm, A. Kirsch-De Mesmaeker, R. Lazzaroni and J.-L. Brédas, Photophysical Properties of Ruthenium(II) Polyazaaromatic Compounds: A Theoretical Insight, *J. Am. Chem. Soc.*, 2004, **126**, 683–692.

33 B. Elias, C. Creely, G. W. Doorley, M. M. Feeney, C. Moucheron, A. Kirsch-DeMesmaeker, J. Dyer, D. C. Grills, M. W. George, P. Matousek, A. W. Parker, M. Towrie and J. M. Kelly, Photooxidation of Guanine by a Ruthenium Dipyridophenazine Complex Intercalated in a Double–Stranded Polynucleotide Monitored Directly by Picosecond Visible and Infrared Transient Absorption Spectroscopy, *Chem. – Eur. J.*, 2008, **14**, 369–375.

34 S. P. Foxon, T. Phillips, M. R. Gill, M. Towrie, A. W. Parker, M. Webb and J. A. Thomas, A Multifunctional Light Switch: DNA Binding and Cleavage Properties of a Heterobimetallic Ruthenium–Rhenium Dipyridophenazine Complex, *Angew. Chem., Int. Ed.*, 2007, **46**, 3686–3688.

35 G. Li, L. Sun, L. Ji and H. Chao, Ruthenium(II) complexes with dppz: from molecular photoswitch to biological applications, *Dalton Trans.*, 2016, **45**, 13261–13276.

36 F. R. Baptista, S. J. Devereux, S. P. Gurung, J. P. Hall, I. V. Sazanovich, M. Towrie, C. J. Cardin, J. A. Brazier, J. M. Kelly and S. J. Quinn, The influence of loops on the binding of the $[Ru(phen)_2\ dppz]^{2+}$ light-switch compound to i-motif DNA structures revealed by time-resolved spectroscopy, *Chem. Commun.*, 2020, **56**, 9703–9706.

37 Y. Jenkins, A. E. Friedman, N. J. Turro and J. K. Barton, Characterization of dipyridophenazine complexes of ruthenium(II): The light switch effect as a function of nucleic acid sequence and conformation, *Biochemistry*, 1992, **31**, 10809–10816.

38 M. Matson, F. R. Svensson, B. Nordén and P. Lincoln, Correlation Between Cellular Localization and Binding Preference to RNA, DNA, and Phospholipid Membrane for Luminescent Ruthenium(II) Complexes, *J. Phys. Chem. B*, 2011, **115**, 1706–1711.

39 R. M. Hartshorn and J. K. Barton, Novel dipyridophenazine complexes of ruthenium(II): exploring luminescent reporters of DNA, *J. Am. Chem. Soc.*, 1992, **114**, 5919–5925.

40 L. Holden, C. S. Burke, D. Cullinane and T. E. Keyes, Strategies to promote permeation and vectorization, and reduce cytotoxicity of metal complex luminophores for bioimaging and intracellular sensing, *RSC Chem. Biol.*, 2021, **2**, 1021–1049.

41 J. Bolger, A. Gourdon, E. Ishow and J.-P. Launay, Stepwise syntheses of mono- and di-nuclear ruthenium tpphz complexes $[(bpy)_2\ Ru(tpphz)]^{2-}$ and $[(bpy)_2\ Ru(tpphz)\ Ru(bpy)_2\ ]^{4+}$ {tpphz = tetrapyrido[3,2-a: 2′,3′-c: 3″,2″-h: 2″,3″′-j]phenazine}, *J. Chem. Soc., Chem. Commun.*, 1995, 1799–1800.

42 J. Bolger, A. Gourdon, E. Ishow and J.-P. Launay, Mononuclear and Binuclear Tetrapyrido[3,2- *a* :2′,3′- *c* :3″,2″- *h* :2‴,3‴- *j*]phenazine (tpphz) Ruthenium and Osmium Complexes, *Inorg. Chem.*, 1996, **35**, 2937–2944.

43 C. Chiorboli, C. A. Bignozzi, F. Scandola, E. Ishow, A. Gourdon and J.-P. Launay, Photophysics of Dinuclear Ru (II) and Os(II) Complexes Based on the Tetrapyrido[3,2- *a*, :2′,3′- *c* :3′ ‘,2′ ‘- *h* :2′ “-3′ “- *j*]phenazine (tpphz) Bridging Ligand, *Inorg. Chem.*, 1999, **38**, 2402–2410.

44 M. Kaufmann, C. Müller, A. A. Cullen, M. P. Brandon, B. Dietzek and M. T. Pryce, Photophysics of Ruthenium(II) Complexes with Thiazole π-Extended Dipyridophenazine Ligands, *Inorg. Chem.*, 2021, **60**, 760–773.

45 S. E. Canton, X. Zhang, J. Zhang, T. B. Van Driel, K. S. Kjaer, K. Haldrup, P. Chabera, T. Harlang, K. Suarez-Alcantara, Y. Liu, J. Pérez, A. Bordage, M. Pápai, G. Vankó, G. Jennings, C. A. Kurtz, M. Rovezzi, P. Glatzel, G. Smolentsev, J. Uhlig, A. O. Dohn, M. Christensen, A. Galler, W. Gawelda, C. Bressler, H. T. Lemke, K. B. Møller, M. M. Nielsen, R. Lomoth, K. Wärnmark and V. Sundström, Toward Highlighting the Ultrafast Electron Transfer Dynamics at the Optically Dark Sites of Photocatalysts, *J. Phys. Chem. Lett.*, 2013, **4**, 1972–1976.

46 M. R. Gill, J. Garcia-Lara, S. J. Foster, C. Smythe, G. Battaglia and J. A. Thomas, A ruthenium(II) polypyridyl complex for direct imaging of DNA structure in living cells, *Nat. Chem.*, 2009, **1**, 662–667.

47 C. Metcalfe and J. A. Thomas, Kinetically inert transition metal complexes that reversibly bind to DNA, *Chem. Soc. Rev.*, 2003, **32**, 215.

48 E. Baggaley, M. R. Gill, N. H. Green, D. Turton, I. V. Sazanovich, S. W. Botchway, C. Smythe, J. W. Haycock, J. A. Weinstein and J. A. Thomas, Dinuclear Ruthenium(II) Complexes as Two–Photon, Time–Resolved Emission

Microscopy Probes for Cellular DNA, *Angew. Chem., Int. Ed.*, 2014, **53**, 3367–3371.

49 M. R. Gill, D. Cecchin, M. G. Walker, R. S. Mulla, G. Battaglia, C. Smythe and J. A. Thomas, Targeting the endoplasmic reticulum with a membrane-interactive luminescent ruthenium(II) polypyridyl complex, *Chem. Sci.*, 2013, **4**, 4512.

50 M. R. Gill, H. Derrat, C. G. W. Smythe, G. Battaglia and J. A. Thomas, Ruthenium(II) Metallo–intercalators: DNA Imaging and Cytotoxicity, *ChemBioChem*, 2011, **12**, 877–880.

51 T. Wilson, P. J. Costa, V. Félix, M. P. Williamson and J. A. Thomas, Structural Studies on Dinuclear Ruthenium (II) Complexes That Bind Diastereoselectively to an Antiparallel Folded Human Telomere Sequence, *J. Med. Chem.*, 2013, **56**, 8674–8683.

52 S. Woitellier, J. P. Launay and C. W. Spangler, Intervalence transfer in pentammineruthenium complexes of .alpha.,. omega.-dipyridyl polyenes, *Inorg. Chem.*, 1989, **28**, 758–762.

53 S. Arounaguiri and B. G. Maiya, "Electro-Photo Switch" and "Molecular Light Switch" Devices Based on Ruthenium(II) Complexes of Modified Dipyridophenazine Ligands: Modulation of the Photochemical Function through Ligand Design, *Inorg. Chem.*, 1999, **38**, 842–843.

54 L. Zedler, A. K. Mengele, K. M. Ziems, Y. Zhang, M. Wächtler, S. Gräfe, T. Pascher, S. Rau, S. Kupfer and B. Dietzek, Unraveling the Light–Activated Reaction Mechanism in a Catalytically Competent Key Intermediate of a Multifunctional Molecular Catalyst for Artificial Photosynthesis, *Angew. Chem., Int. Ed.*, 2019, **58**, 13140–13148.

55 N. Kosiol, S. Juranek, P. Brossart, A. Heine and K. Paeschke, G-quadruplexes: a promising target for cancer therapy, *Mol. Cancer*, 2021, **20**, 40.

56 J. Spiegel, S. Adhikari and S. Balasubramanian, The Structure and Function of DNA G-Quadruplexes, *Trends Chem.*, 2020, **2**, 123–136.

57 C. Yang, Q. Zhou, Z. Jiao, H. Zhao, C.-H. Huang, B.-Z. Zhu and H. Su, Ultrafast excited state dynamics and light-switching of [Ru(phen)2(dppz)]2+ in G-quadruplex DNA, *Commun. Chem.*, 2021, **4**, 68.

58 R. Hänsel-Hertsch, D. Beraldi, S. V. Lensing, G. Marsico, K. Zyner, A. Parry, M. Di Antonio, J. Pike, H. Kimura, M. Narita, D. Tannahill and S. Balasubramanian, G-quadruplex structures mark human regulatory chromatin, *Nat. Genet.*, 2016, **48**, 1267–1272.

59 R. Hänsel-Hertsch, J. Spiegel, G. Marsico, D. Tannahill and S. Balasubramanian, Genome-wide mapping of endogenous G-quadruplex DNA structures by chromatin immunoprecipitation and high-throughput sequencing, *Nat. Protoc.*, 2018, **13**, 551–564.

60 R. Hänsel-Hertsch, A. Simeone, A. Shea, W. W. I. Hui, K. G. Zyner, G. Marsico, O. M. Rueda, A. Bruna, A. Martin, X. Zhang, S. Adhikari, D. Tannahill, C. Caldas and S. Balasubramanian, Landscape of G-quadruplex DNA structural regions in breast cancer, *Nat. Genet.*, 2020, **52**, 878–883.

61 C. Ribeyre, J. Lopes, J.-B. Boulé, A. Piazza, A. Guédin, V. A. Zakian, J.-L. Mergny and A. Nicolas, The Yeast Pif1 Helicase Prevents Genomic Instability Caused by G-Quadruplex-Forming CEB1 Sequences In Vivo, *PLoS Genet.*, 2009, **5**, e1000475.

62 K. Paeschke, M. L. Bochman, P. D. Garcia, P. Cejka, K. L. Friedman, S. C. Kowalczykowski and V. A. Zakian, Pif1 family helicases suppress genome instability at G-quadruplex motifs, *Nature*, 2013, **497**, 458–462.

63 M. M. Makowski, C. Gräwe, B. M. Foster, N. V. Nguyen, T. Bartke and M. Vermeulen, Global profiling of protein–DNA and protein–nucleosome binding affinities using quantitative mass spectrometry, *Nat. Commun.*, 2018, **9**, 1653.

64 S. Shi, X. Geng, J. Zhao, T. Yao, C. Wang, D. Yang, L. Zheng and L. Ji, Interaction of [Ru(bpy)2(dppz)]2+ with human telomeric DNA: Preferential binding to G-quadruplexes over i-motif, *Biochimie*, 2010, **92**, 370–377.

65 C. Rajput, R. Rutkaite, L. Swanson, I. Haq and J. A. Thomas, Dinuclear Monointercalating Ru^{II} Complexes That Display High Affinity Binding to Duplex and Quadruplex DNA, *Chem. – Eur. J.*, 2006, **12**, 4611–4619.

66 K. Li, L. Yatsunyk and S. Neidle, Water spines and networks in G-quadruplex structures, *Nucleic Acids Res.*, 2021, **49**, 519–528.

67 G. Piraux, L. Bar, M. Abraham, T. Lavergne, H. Jamet, J. Dejeu, L. Marcélis, E. Defrancq and B. Elias, New Ruthenium–Based Probes for Selective G–Quadruplex Targeting, *Chem. – Eur. J.*, 2017, **23**, 11872–11880.

68 E. Wachter, D. Moyá, S. Parkin and E. C. Glazer, Ruthenium Complex "Light Switches" that are Selective for Different G–Quadruplex Structures, *Chem. – Eur. J.*, 2016, **22**, 550–559.

69 K. T. McQuaid, S. Takahashi, L. Baumgaertner, D. J. Cardin, N. G. Paterson, J. P. Hall, N. Sugimoto and C. J. Cardin, Ruthenium Polypyridyl Complex Bound to a Unimolecular Chair-Form G-Quadruplex, *J. Am. Chem. Soc.*, 2022, **144**, 5956–5964.

70 L. Holden, K. S. Gkika, C. S. Burke, C. Long and T. E. Keyes, Selective, Disruptive Luminescent Ru(II) Polypyridyl Probes of G-Quadruplex, *Inorg. Chem.*, 2023, **62**, 2213–2227.

71 A. Chettri, H. D. Cole, J. A. Roque III, K. R. A. Schneider, T. Yang, C. G. Cameron, S. A. McFarland and B. Dietzek-Ivanšić, Interaction with a Biomolecule Facilitates the Formation of the Function-Determining Long-Lived Triplet State in a Ruthenium Complex for Photodynamic Therapy, *J. Phys. Chem. A*, 2022, **126**, 1336–1344.

72 I. Kejnovská, D. Renčiuk, J. Palacký and M. Vorlíčková, in *G-Quadruplex Nucleic Acids*, ed. D. Yang and C. Lin, Springer New York, New York, NY, 2019, vol. 2035, pp. 25–44.

73 S.R. Gallagher, Quantitation of DNA and RNA with Absorption and Fluorescence Spectroscopy, *Curr. Protoc. Immunol.*, 2017, **116**, A.3L.1–A.3L.14.

74 R. Siebert, D. Akimov, M. Schmitt, A. Winter, U. S. Schubert, B. Dietzek and J. Popp, Spectroscopic Investigation of the Ultrafast Photoinduced Dynamics in π-Conjugated Terpyridines, *ChemPhysChem*, 2009, **10**, 910–919.

75 M. Karnahl, C. Kuhnt, F. Ma, A. Yartsev, M. Schmitt, B. Dietzek, S. Rau and J. Popp, Tuning of Photocatalytic Hydrogen Production and Photoinduced Intramolecular Electron Transfer Rates by Regioselective Bridging Ligand Substitution, *ChemPhysChem*, 2011, **12**, 2101–2109.

76 S. Fantacci, F. De Angelis, A. Sgamellotti and N. Re, A TDDFT study of the ruthenium(II) polyazaaromatic complex [Ru(dppz)(phen)2]2+ in solution, *Chem. Phys. Lett.*, 2004, **396**, 43–48.

77 A. C. Bhasikuttan, M. Suzuki, S. Nakashima and T. Okada, Ultrafast Fluorescence Detection in Tris(2,2′-bipyridine) ruthenium(II) Complex in Solution: Relaxation Dynamics Involving Higher Excited States, *J. Am. Chem. Soc.*, 2002, **124**, 8398–8405.

78 N. H. Damrauer, G. Cerullo, A. Yeh, T. R. Boussie, C. V. Shank and J. K. McCusker, Femtosecond Dynamics of Excited-State Evolution in $[Ru(bpy)_3]^{2+}$, *Science*, 1997, **275**, 54–57.

79 H. Yamamoto, *Topics in Current Chemistry*, 2007, **269**.

80 K. Peuntinger, T. D. Pilz, R. Staehle, M. Schaub, S. Kaufhold, L. Petermann, M. Wunderlin, H. Görls, F. W. Heinemann, J. Li, T. Drewello, J. G. Vos, D. M. Guldi and S. Rau, Carbene based photochemical molecular assemblies for solar driven hydrogen generation, *Dalton Trans.*, 2014, **43**, 13683–13695.

81 S. Tschierlei, M. Presselt, C. Kuhnt, A. Yartsev, T. Pascher, V. Sundström, M. Karnahl, M. Schwalbe, B. Schäfer, S. Rau, M. Schmitt, B. Dietzek and J. Popp, Photophysics of an Intramolecular Hydrogen–Evolving Ru–Pd Photocatalyst, *Chem. – Eur. J.*, 2009, **15**, 7678–7688.

82 A. Marchand and V. Gabelica, Folding and misfolding pathways of G-quadruplex DNA, *Nucleic Acids Res.*, 2016, **44**, 10999–11012.

83 F. D'Aria, V. M. D'Amore, F. S. Di Leva, J. Amato, M. Caterino, P. Russomanno, S. Salerno, E. Barresi, M. De Leo, A. M. Marini, S. Taliani, F. Da Settimo, G. F. Salgado, L. Pompili, P. Zizza, S. Shirasawa, E. Novellino, A. Biroccio, L. Marinelli and C. Giancola, Targeting the KRAS oncogene: Synthesis, physicochemical and biological evaluation of novel G-Quadruplex DNA binders, *Eur. J. Pharm. Sci.*, 2020, **149**, 105337.

84 F. E. Poynton, J. P. Hall, P. M. Keane, C. Schwarz, I. V. Sazanovich, M. Towrie, T. Gunnlaugsson, C. J. Cardin, D. J. Cardin, S. J. Quinn, C. Long and J. M. Kelly, Direct observation by time-resolved infrared spectroscopy of the bright and the dark excited states of the $[Ru(phen)_2(dppz)]^{2+}$ light-switch compound in solution and when bound to DNA, *Chem. Sci.*, 2016, **7**, 3075–3084.

85 C. J. Cardin, J. M. Kelly and S. J. Quinn, Photochemically active DNA-intercalating ruthenium and related complexes – insights by combining crystallography and transient spectroscopy, *Chem. Sci.*, 2017, **8**, 4705–4723.

86 T. Wilson, M. P. Williamson and J. A. Thomas, Differentiating quadruplexes: binding preferences of a luminescent dinuclear ruthenium(II) complex with four-stranded DNA structures, *Org. Biomol. Chem.*, 2010, **8**, 2617.

87 S. Shi, J. Zhao, X. Geng, T. Yao, H. Huang, T. Liu, L. Zheng, Z. Li, D. Yang and L. Ji, Molecular "light switch" for G-quadruplexes and i-motif of human telomeric DNA: [Ru(phen)2(dppz)]2+, *Dalton Trans.*, 2010, **39**, 2490.

88 A. Marchand, A. Granzhan, K. Iida, Y. Tsushima, Y. Ma, K. Nagasawa, M.-P. Teulade-Fichou and V. Gabelica, Ligand-Induced Conformational Changes with Cation Ejection upon Binding to Human Telomeric DNA G-Quadruplexes, *J. Am. Chem. Soc.*, 2015, **137**, 750–756.

89 A. Ghosh, M. Trajkovski, M. Teulade-Fichou, V. Gabelica and J. Plavec, Phen–DC_3 Induces Refolding of Human Telomeric DNA into a Chair–Type Antiparallel G–Quadruplex through Ligand Intercalation, *Angew. Chem.*, 2022, **134**, e202207384.

90 E. J. C. Olson, D. Hu, A. Hörmann, A. M. Jonkman, M. R. Arkin, E. D. A. Stemp, J. K. Barton and P. F. Barbara, First observation of the key intermediate in the 'light-switch' mechanism of [Ru(phen)2dppz]2+, *Chemtracts*, 1998, **11**, 377–384.